

PACS numbers: 42.65.Hw; 42.65.Jx; 42.65.Wi; 42.65.Re; 42.68.Ay
DOI: 10.1070/QE2009v039n06ABEH014012

Femtosecond filaments as a new type of laser guide stars for astronomical adaptive optics

N.A. Panov, A.D. Savvin, O.G. Kosareva, A.B. Savel'ev-Trofimov,
V.P. Kandidov, S.A. Potanin, S.D. Pol'skikh

***Abstract*. A method for creating laser guide stars based on filaments of high-power femtosecond radiation at altitudes more than 10 km is proposed. The parameters of femtosecond laser pulses optimal for the formation of laser guide stars are determined. An analytic expression for the critical self-focusing power on a vertical path is obtained.**

Keywords: *laser guide star, femtosecond pulse, filament.*

1. Introduction

When the power of femtosecond laser pulses propagating in the atmosphere exceeds the critical self-focusing power (~ 5 GW for 800-nm pulses), one or several extended thin filaments are produced due to the self-compression of the laser beam caused by Kerr self-focusing [1, 2]. When the laser beam intensity achieves $\sim 5 \times 10^{13}$ W cm^{-2} [3], its increase ceases due to multiphoton ionisation of a medium resulting in the scattering and absorption of the laser pulse energy.

The filamentation of high-power femtosecond laser pulses in the atmosphere is accompanied by a considerable spectral broadening (up to 250 nm [4] and 4500 nm [5] in the short- and long-wavelength spectral regions, respectively), which is called the supercontinuum (or white light) generation. The supercontinuum radiation propagates predominantly forward along the filament axis, both in the long- and short-wavelength spectral regions. The short-wavelength radiation is also observed in the form of interfering conical emission diverging from each of the filaments [6]. The cone angle of this radiation is $\sim 0.1^\circ$ [2, 7].

The plasma channels of filaments with the lifetime ~ 10 ns [8] fluoresce in the optical range, their emission spectrum changing qualitatively with time [9]. Thus, at times up to 1 ns, the emission of molecular nitrogen N_2 and singly ionised nitrogen N_2^+ dominates, in the range from 1 to 10 ns – the thermal emission continuum of electrons in a plasma, and in the range from 10 to 1000 ns – the emission of atomic oxygen and nitrogen. Laboratory experiments [10] have demonstrated the amplification of spontaneous emission of N_2 and N_2^+ due to population inversion induced in a medium by femtosecond radiation. This leads to the predominant propagation of radiation along a filament, in particular, in the direction opposite to the laser beam propagation.

Experiments [11] showed the possibility to observe fluorescence of molecular or singly ionised nitrogen from a distance of ~ 100 m. Methods were proposed for increasing fluorescence signals by scaling output laser beams [12, 13], their focusing [14], diaphragming [15], chirping [16], etc.

The supercontinuum emission [17] and fluorescence of plasma channels [18] can be used for remote ecological monitoring of the environment. Thus, the absorption lines of water were recorded from an altitude of 5 km against the filament emission background [17]. During the propagation of 20-J, 500-fs pulses, the emission of filaments was visible to the naked eye [19]. The filamentation of high-power femtosecond laser radiation in atmosphere can be also used to initiate an atmospheric electricity discharge [20] and for the propagation of microwave signals along plasma channels in filaments [21, 22].

In this paper, we propose to use the emission of filament plasma channels as new laser guide stars [23] for astronomical adaptive optics. A laser guide star is an artificial star-like source formed in the upper atmospheric layers. Its radiation propagating through the turbulent atmosphere contains information on perturbations of the refractive index, which can be further used to compensate for turbulent distortions by using an adaptive optics system.

By now two methods for creating laser guide stars are realised. In the first method, sodium atoms at altitudes ~ 100 km are excited by laser radiation at 589.2 nm [24]. The excited atoms emit isotropic radiation at the same wavelength, scattering in this way laser radiation. A small part of this radiation scattered backward represents a star-like source. The second method uses the Rayleigh scattering of laser radiation in the atmosphere at altitudes of ~ 15 km [25]. Because Rayleigh scattering is most intense at short wavelengths, laser radiation with the shortest wavelength, which is still transmitted in the atmosphere, is used.

Both these methods are linear, i.e. the brightness of the laser guide star is proportional to the laser radiation

N.A. Panov, A.D. Savvin, O.G. Kosareva, A.B. Savel'ev-Trofimov, V.P. Kandidov Department of Physics, International Laser Center, M.V. Lomonosov Moscow State University, Vorob'evy gory, 119991 Moscow, Russia; e-mail: panov_na@mail.ru;
S.A. Potanin M.V. Lomonosov Moscow State University, P.K. Shternberg State Astronomical Institute, M.V. Lomonosov Moscow State University, Vorob'evy gory, 119991 Moscow, Russia;
S.D. Pol'skikh Astrofizika Research and Production Association, Volokolamskoe sh. 95, 125424 Moscow, Russia

Received 28 November 2008
Kvantovaya Elektronika **39** (6) 560 – 565 (2009)
Translated by M.N. Sapozhnikov

intensity. As a result, these stars are rather weak because to obtain a star of brightness sufficient for the operation of a wave-front sensor (10th stellar magnitude [26]), high-power cw lasers of powers tens kilowatts are required [26].

Filament guide stars offer a number of advantages over sodium [24] and Rayleigh [25] sources. The method for creating laser guide stars proposed in our paper is substantially nonlinear and has a distinct exciting pulse power threshold beginning from which the self-compression of the laser beam occurs accompanied by plasma formation. A strong absorption of energy during the multiphoton ionisation of the medium results in the energy supply to the plasma amounting to 10 % of the pulse energy [16], which is usually equal to tens and hundreds of millijoules [11, 27, 28].

The 10-μJ radiation pulses with a repetition rate of 1 kHz (10 mW of average power scattered to the total sphere) scattered from an altitude of 15 km correspond to a laser guide star of the 7th stellar magnitude. Because the energy absorbed during multiphoton ionisation is a few–tens of millijoules, we can expect that a laser guide star can be created that will be brighter by several stellar magnitudes. In addition, the predominant backward scattering due to amplification of spontaneous emission of N_2 and N_2^+ can enhance the brightness of the laser guide star up to the values that are inaccessible by other methods.

To provide the satisfactory compensation of turbulence, a laser system for generation of laser guide stars together with an adaptive optics system should operate at pulse repetition rates ~ 100 Hz and higher [23]. At present terawatt and subterawatt femtosecond laser systems with such repetition rates are developed and used. Thus, a laser system generating terawatt pulses at a repetition rate of 1 kHz was developed in [29].

In this connection it is important to optimise the parameters of femtosecond laser pulses over the wavelength and the beam diameter at the output aperture for creating filament guide stars with the maximal brightness at altitudes above 10 km. This is the aim of our work.

2. Mathematical model of the formation of a filament of a high-power femtosecond pulse on a vertical path

Filamentation on vertical atmospheric paths of length of the order of 1 km and more does not differ qualitatively from filamentation on horizontal paths, but has, however, a number of features related to the altitude dependences of the atmosphere density and the structural constant of the atmospheric turbulence. The Kerr nonlinearity coefficient n_2 is proportional to the concentration N_a of molecules in air.

The simplest approximation describing the decrease in the air density with altitude is the barometric formula derived in the isothermal atmosphere approximation. The filamentation of high-power femtosecond radiation on vertical paths with such a dependence of the air density on the altitude was numerically investigated in [30].

There also exist more accurate empirical dependences of the air density on the altitude above the earth surface. Thus, the dependences of the air temperature T and pressure p on the altitude z presented in [31] have the form

$$T(z) = 15.04 - 0.00649z,$$

$$p(z) = 1.1977 \times 10^{-11}(T(z) + 273.1)^{5.256} \quad (1)$$

for $z < 11000$ m (troposphere) and

$$T(z) = -56.46,\ p(z) = 22.65\exp(1.73 - 0.000157z) \quad (2)$$

for $z > 11000$ m (stratosphere). Temperature in (1) and (2) is measured in degrees Celsius, pressure – in kilopascals, and altitude – in metres. Knowing $T(z)$ and $p(z)$, the expression for concentration is simply obtained from the Mendeleev–Clapeyron equation:

$$N_a(z) = \frac{7.238 \times 10^{19} p(z)}{T(z) + 273.1}, \quad (3)$$

where $N_a(z)$ is measured in cm^{-3}. We will describe the dependence of the concentration of air molecules on the altitude by using relations (1)–(3). Figure 1a presents the dependence $N_a(z)$ according to model (1)–(3).

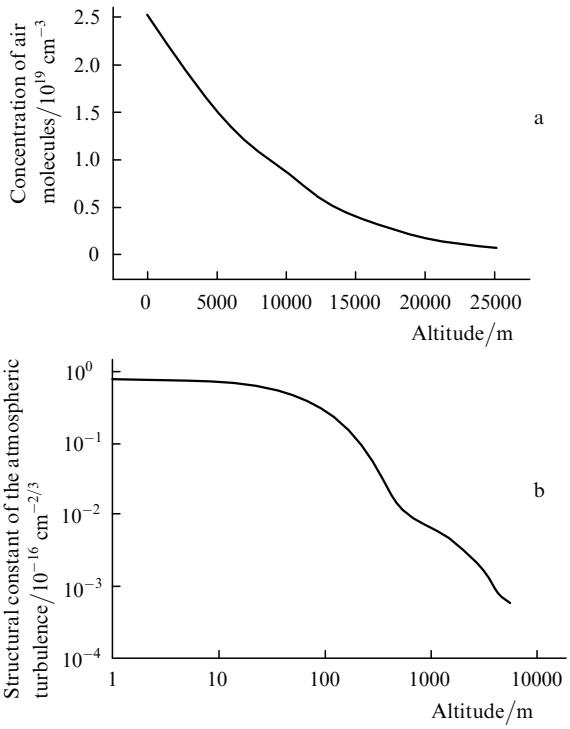

Figure 1. Dependences of the concentration of air molecules (a) and the structural constant of the atmospheric turbulence (b) on the altitude.

The structural constant C_n^2 of fluctuations of the refractive index also strongly depends on the altitude above the earth surface. The processing of experimental data allowed the formulation of several models of dependences $C_n^2(z)$. The most popular of them are the day and night submarine laser communication (SLC) models [32] and the Hufnagel–Valley model [32]. These models are qualitatively similar, both predicting the decrease in the structural constant C_n^2 with increasing altitude. Because the Hufnagel–Valley dependence is a continuous function of the altitude, we will use this dependence to simulate filamentation on vertical paths.

According to the Hufnagel–Valley model, the structural constant is described by the expression

$$C_n^2(z) = 0.00594\left(\frac{V(z)}{27}\right)^2 (10^{-5}z)^{10}\exp\left(-\frac{z}{1000}\right) + 2.7\times 10^{-16}\exp\left(-\frac{z}{1500}\right) + C_n^2(z=0)\exp\left(-\frac{z}{100}\right), \quad (4)$$

where the structural constant of the atmospheric turbulence at sea level is $C_n^2(z=0) = 1.7\times 10^{-14}$ m$^{-2/3}$. This value is chosen to obtain agreement with the day SLC model. In (4),

$$V(z) = \frac{1}{1.5\times 10^4}\int_{5\times 10^3}^{2\times 10^4}\tilde{V}^2(z)\mathrm{d}z, \qquad \tilde{V}(z) = 30\exp\left[-\left(\frac{z-9400}{4800}\right)^2\right]. \quad (5)$$

and C_n^2 is measured in m$^{-2/3}$ and z in metres. The plot $C_n^2(z)$ is shown in Fig. 1b.

To analyse the initial stage of filamentation on vertical atmospheric paths, when the influence of nonstationary defocusing in a self-induced laser plasma is negligible, the equation for the slowly varying complex amplitude E of the electric field can be written in the form

$$2ik_0\frac{\partial E}{\partial z} = \Delta_\perp E + 2k_0^2\left(\frac{n_2(z)|E|^2}{2} + \Delta n_{\mathrm{turb}}(x,y,z)\right)E, \quad (6)$$

where $k_0 = 2\pi/\lambda_0$ and λ_0 is the central radiation wavelength. The dependence $n_2(z)$ is determined by the expression

$$n_2(z) = n_2(z=0)[N_\mathrm{a}(z)/N_\mathrm{a}(z=0)], \quad (7)$$

where $N_\mathrm{a}(z=0) = 2.7\times 10^{19}$ cm^{-3}. Turbulent fluctuations of the refractive index are taken into account by the term Δn_{turb} in (6), which is determined by using the algorithm presented in [33]. The value of Δn_{turb} was calculated by using the modified von Karman spectrum [34] with the external and internal scales of the atmospheric turbulence $L_0 = 1$ m and $l_0 = 1$ mm, respectively. We will use the initial conditions in the form of a Gaussian beam

$$E(x,y,z=0) = E_0\exp\left[-\frac{x^2+y^2}{2a_0^2}\right], \quad (8)$$

where E_0 is related to the peak pulse power P_0 by the expression

$$E_0 = \sqrt{\frac{8P_0}{ca_0^2}}. \quad (9)$$

Here, a_0 is the beam radius and c is the speed of light in vacuum.

3. Optimisation of radiation parameters for creating a filament guide star at altitudes above 10 km

To optimise the distance at which a filament is formed during the propagation of a high-power femtosecond laser pulse in the atmosphere, we will find the critical self-focusing power on a vertical path in the model atmosphere without turbulence. To do this, we assume that $\Delta n_{\mathrm{turb}} = 0$ in (6).

The critical power and self-focusing length on the vertical path were determined by solving equation (6) with radii a_0 from 1 to 9 cm and peak powers P_0 from 1 to $30P_{\mathrm{cr}}^0$, where P_{cr}^0 is the critical self-focusing power on the horizontal path [35]:

$$P_{\mathrm{cr}}^0 = \frac{3.77\lambda_0^2}{8\pi n_2(\lambda_0)}. \quad (10)$$

The critical self-focusing power decreases on passing to the shorter-wavelength region due to the decrease in λ_0 and increase in n_2 [36]. For example, as the wavelength is decreased from 800 to 400 nm, the critical self-focusing power on the horizontal path decreases approximately by an order of magnitude.

A step in the change of radius a_0 was 1 mm and a step over the peak power was $0.2P_{\mathrm{cr}}^0$. At low powers, the pulse did not collapse (by a collapse is meant the increase in the pulse initial intensity by two orders of magnitude), its peak intensity achieved a maximum value and then began to decrease. At high powers, such a nonmonotonic change in the peak intensity was absent, and power at which a change in the pulse propagation regimes occurred was treated as the critical self-focusing power $P_{\mathrm{cr}}(a_0)$ for the given beam radius.

Figures 2a and b present the dependences of the critical self-focusing power on the vertical path on the beam radius for central wavelengths $\lambda_0 = 800$ and 400 nm. The results of the numerical experiment are presented by the black circles. As expected, the critical power increases with increasing the beam radius. The open circles in Fig. 2 correspond to the obvious limiting case $P_{\mathrm{cr}}(a_0) \to P_{\mathrm{cr}}^0$ for $a_0 \to 0$. This is explained by the fact that beams of very small radius propagate in the surface atmospheric layer, and a filament has time to form in a medium with a constant density $N_\mathrm{a}(z=0)$.

The results of the numerical calculation of the critical self-focusing power were approximated by the expression

$$P_{\mathrm{cr}}^{\mathrm{app}}(a_0) = P_{\mathrm{cr}}^0\left[1 + (A + Ba_0)^3\right], \quad (11)$$

where a_0 is measured in centimetres. Constants A and B were determined with an accuracy of 3 %. Note that the approximation was performed only for data obtained in the numerical experiment. Nevertheless, expression (11) for $a_0 = 0$ gives the value $P_{\mathrm{cr}}^{\mathrm{app}}(a_0)$ that differs from the limiting value $P_{\mathrm{cr}}(a_0 \to 0) \to P_{\mathrm{cr}}^0$ by no more than 10 %. This demonstrates the good quality of approximation (11).

The values of constants A and B for the wavelengths used in modern high-power femtosecond laser systems are presented in Table 1. Table 1 shows that constant A weakly depends on λ_0, its average value being 0.457. The value of B depends on λ_0 rather strongly. This dependence can be approximated quite accurately by the expression $B = 5.60/\sqrt{\lambda_0}$, where λ_0 is measured in nanometres. Thus, the critical self-focusing power $P_{\mathrm{cr}}^{\mathrm{app}}$ (11) on the vertical path as a function of the beam radius a_0 at the laser system output can be written in the form

$$P_{\mathrm{cr}}^{\mathrm{app}}(a_0,\lambda_0) = P_{\mathrm{cr}}^0\left\{1 + \left[0.457 + \frac{5.60}{\sqrt{\lambda_0}}\,a_0\right]^3\right\}. \quad (12)$$

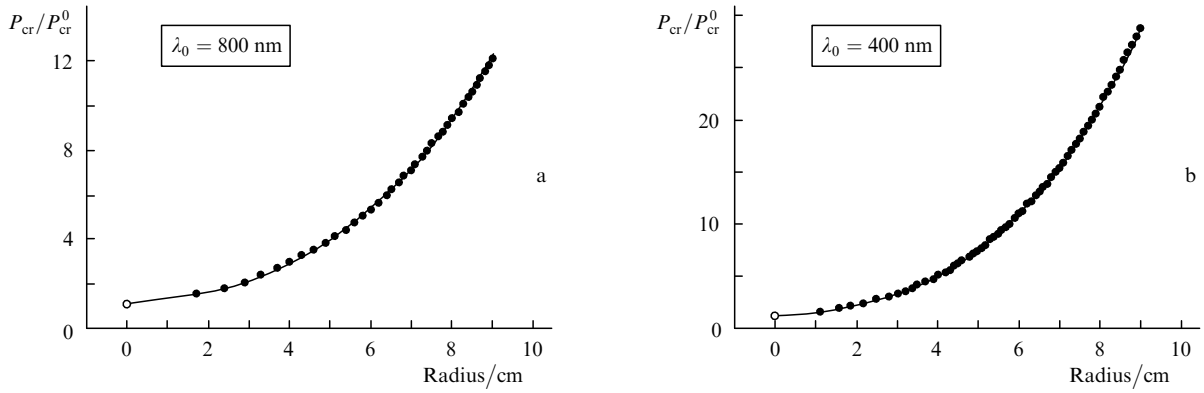

Figure 2. Dependences of the critical self-focusing power on the vertical path on the output laser beam radius. The black circles are the numerical experiment; open circles correspond to the limiting case $P_{cr}(a_0 \to 0) \to P_{cr}^0$; solid curves are approximations of experimental data by dependence (11).

Table 1. Constants entering expression (1) for different wavelengths.

Laser system	λ_0/nm	A	B/cm^{-1}
Ti : sapphire, second harmonic	400	0.450	0.284
Ti : sapphire	800	0.447	0.197
Nd^{3+}	1060	0.471	0.170
Cr : F	1260	0.459	0.155

To create filament guide stars at altitudes about 10 km, laser pulses of power exceeding the value determined by approximation (12) should be used.

Figure 3 presents the dependences of the distance z_{sf} of the filamentation onset on the power P_0 of a high-power femtosecond pulse propagating along the vertical atmospheric path. As in the case of propagation along the horizontal path, the self-focusing distance increases with decreasing the peak pulse power. For the same excess of the peak pulse power over the critical self-focusing power, the distance at which a filament is formed increases with decreasing the wavelength. According to the Marburger formula [35], determining the formation of a filament on the horizontal path, the distance z_{sf} increases proportionally to λ_0^{-1}. In the case of filamentation on the vertical path, the value of z_{sf} increases faster because the Kerr nonlinearity coefficient decreases with the altitude. A filament guide star at altitudes above 10 km can be created for the laser beam radius $a_0 > 5$ cm and $\lambda_0 = 400$ nm and for $a_0 > 6$ cm and $\lambda_0 = 800$ nm.

Because turbulent fluctuations of the refractive index of air considerably affect the filamentation of high-power femtosecond pulses propagating along vertical and hori-

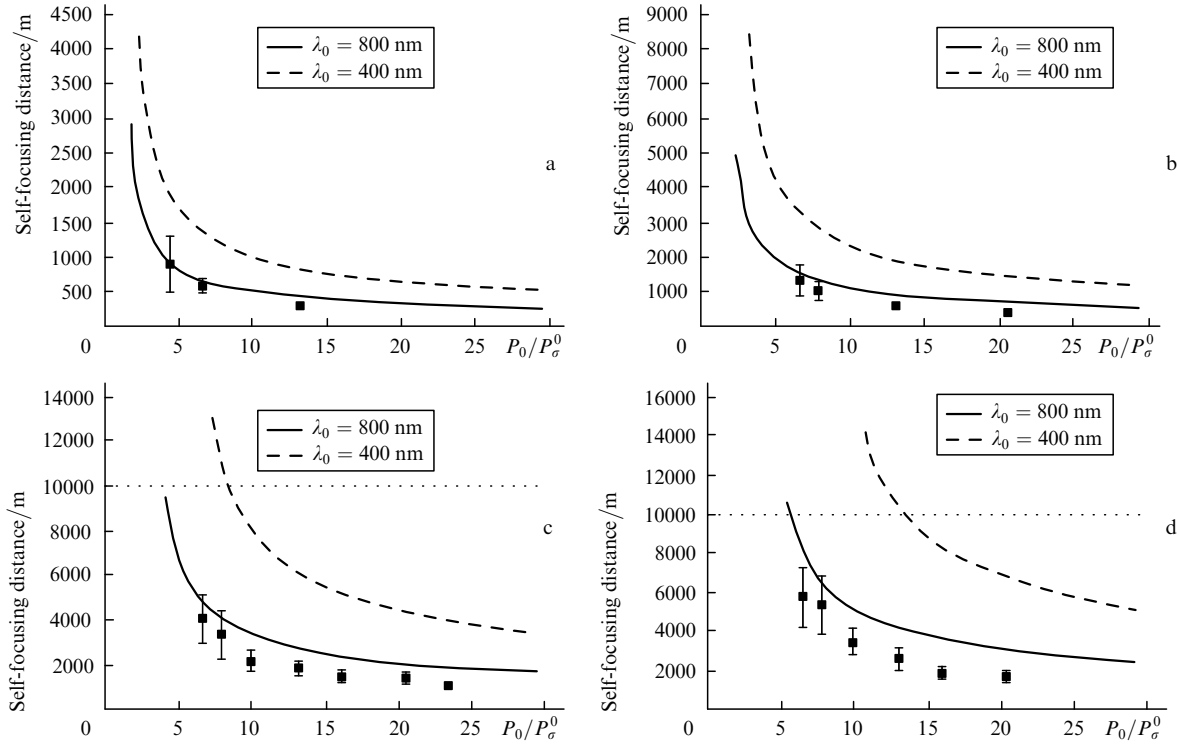

Figure 3. Dependences of the altitude of formation of a filament guide star on the peak pulse power for the beam radii 2 (a), 3 (b), 5 (c), and 6 cm (d). The solid and dashed curves correspond to calculations in the absence of turbulence, the squares with error bars – to calculations in the turbulent atmosphere.

zontal atmospheric paths (in particular, they produce multiple filamentation [33]), they should be taken into account by analysing filamentation. In expression (6), they are described by the term $\Delta n_{\rm turb}$.

The squares with error bars in Fig. 3 present the results of the numerical experiment on determining the self-focusing distance in the turbulent atmosphere for the central wavelength $\lambda_0 = 800$ nm. The error is defined as the standard deviation of the filament position for 20 different realisations of turbulent phase screens. One can easily see that the self-focusing distance in the turbulent atmosphere is smaller than in the atmosphere without turbulence. In addition, the measurement error of this distance increases with decreasing the peak pulse power. For example, for $a_0 = 5$ cm and $P_0/P_{\rm cr}^0 = 20.5$, the self-focusing distance is $z_{\rm sf} = 1310 \pm 180$ m, while for $P_0/P_{\rm cr}^0 = 6.5$, this distance is $z_{\rm sf} = 4100 \pm 1100$ m, i.e. the accuracy of positioning the filament onset decreases from 13 % to 27 %.

Due to the decrease in the positioning accuracy, the approximation (12) of the dependence of the critical self-focusing power on the vertical path on the beam radius becomes very important. If this power only slightly exceeds the critical self-focusing power for the given radius, a filament is formed but the accuracy of its onset positioning is small. The critical self-focusing power on the vertical path for a beam of radius 5 cm for $\lambda_0 = 800$ nm is $P_{\rm cr}^{\rm app} = 4.1 P_{\rm cr}^0$. If $P_0/P_{\rm cr}^0 = 6.5$, which corresponds to a small positioning accuracy, then $P_0/P_{\rm cr}^{\rm app} = 1.6$, i.e. the excess of the peak pulse power over the critical self-focusing power is rather small. The satisfactory positioning accuracy of about 10 % is achieved for $P_0/P_{\rm cr}^{\rm app} > 3$.

As the radiation wavelength is decreased and the filamentation onset is removed from the laser system output, the laser plasma is generated more efficiently, resulting in a greater brightness of the laser guide star. This is rigorously shown in [36], although this also follows from simple intuitive considerations. Indeed, to ionise nitrogen molecules by radiation at 800 nm, 11 photons are required. As the wavelength is decreased to 400 nm, the number of photons required for ionisation is reduced to six. This leads to the increase in the ionisation probability by several orders of magnitude. However, the wavelength should exceed 300 nm because the transparency of the atmosphere below this wavelength drastically decreases due to the absorption of UV radiation by ozone O_3 [37].

4. Conclusions

Laser guide stars can be created upon filamentation of high-power femtosecond laser pulses in the atmosphere at altitudes above 10 km during the propagation of a beam of radius more than 5 cm with the critical power exceeding the critical self-focusing power on the vertical path by three times and more [see (12)]. In this case, the most efficient are pulses at the wavelength only slightly more than 300 nm.

In this connection of interest are the filaments of the 400-nm second-harmonic pulses of a Ti : sapphire laser, which can be generated with the efficiency achieving to a few tens percent [38, 39]. In addition, it is expected that bright filament guide stars at a wavelength of 351 nm will be created. Such radiation can be produced by generating the third harmonic of a 1040 – 1060-nm femtosecond ytterbium-doped fibre laser [40] amplified in a XeF excimer system similarly to [41].

The authors have failed to obtain a simple approximation for the dependence of the self-focusing distance on the vertical path on the beam radius a_0 and pulse power P_0, which would have the asymptotics described by the Marbueger formula [35] in the limiting case $a_0 \to 0$. This important applied problem is being solved at present.

Acknowledgements. This work was supported by the Russian Foundation for Basic Research (Grant Nos 07-02-12049-ofi and 09-02-01200-a).

References

1. Braun A., Korn G., Liu X., Du D., Squier J., Mourou G. *Opt. Lett.*, **20**, 73 (1995).
2. Nibbering E.T.J., Curley P.F., Grillon G., Prade B.S., Franco M.A., Salin F., Mysyrowicz A. *Opt. Lett.*, **21**, 62 (1996).
3. Kasparian J., Sauerbrey R., Chin S.L. *Appl. Phys. B*, **71**, 877 (2000).
4. Théberge F., Liu W., Luo Q., Chin S.L. *Appl. Phys. B*, **80**, 221 (2005).
5. Kasparian J., Sauerbrey R., Mondelain D., Niedermeier S., Yu J., Wolf J.-P., André Y.-B., Franco M., Prade B., Tzortzakis S., Mysyrowicz A., Rodriguez M., Wille H., Wöste L. *Opt. Lett.*, **25**, 1397 (2000).
6. Liu W., Hosseini S.A., Luo Q., Ferland B., Chin S.L., Kosareva O.G., Panov N.A., Kandidov V.P. *New J. Phys.*, **6**, 6.1 (2004).
7. Kosareva O.G., Kandidov V.P., Brodeur A., Chien C.Y., Chin S.L. *Opt. Lett.*, **22**, 1332 (1997).
8. Tzortzakis S., Prade B., Franco M., Mysyrowicz A. *Opt. Commun.*, **181**, 123 (2000).
9. Martin F., Mawassi R., Vidal F., Gallimberti I., Comtois D., Petin H., Kieffer J.C., Mercure H.P. *Appl. Spectroscopy*, **56**, 1444 (2002).
10. Luo Q., Liw W., Chin S.L. *Appl. Phys. B*, **76**, 337 (2003).
11. Hosseini S.A., Luo Q., Ferland B., Liu W., Chin S.L., Kosareva O.G., Panov N.A., Aközbek N., Kandidov V.P. *Phys. Rev. A*, **70**, 033802 (2004).
12. Luo Q., Hosseini S.A., Liu W., Gravel J.-F., Kosareva O.G., Panov N.A., Aközbek N., Kandidov V.P., Roy G., Chin S.L. *Appl. Phys. B*, **80**, 35 (2004).
13. Kosareva O.G., Panov N.A., Aközbek N., Kandidov V.P., Luo Q., Hosseini S.A., Liu W., Gravel J.-F., Roy G., Chin S.L. *Appl. Phys. B*, **82**, 111 (2006).
14. Théberge F., Liu W., Hosseni S.A., Luo Q., Sarifi S.M., Chin S.L. *Appl. Phys. B*, **81**, 131 (2005).
15. Daigle J.-F., Kosareva O., Panov N., Begin M., Lessard F., Marceau C., Kamali Y., Roy G., Kandidov V.P., Chin S.L. *Appl. Phys. B*, **94**, 249 (2009).
16. Panov N.A., Kosareva A.G., Kandidov V.P., Akosbek N., Skalora M., Chin S.L. *Kvantovaya Elektron.*, **37**, 1153 (2007) [*Quantum Electron.*, **37**, 1153 (2007)].
17. Kasparian J., Rodrigues M., Mejean G., Yu J., Salmon E., Wille H., Bourayou R., Frey S., Andre Y.-B., Mysyrowicz A., Sauerbrey R., Wolf J.-P., Woste L. *Science*, **301**, 61 (2003).
18. Luo Q., Xu H.L., Hosseni S.A., Daigle J.-F., Théberge F., Sarifi S.M., Chin S.L. *Appl. Phys. B*, **82**, 105 (2006).
19. Béjot P., Bonacina L., Extermann J., Moret M., Wolf J.P., Ackermann R., Lascoux N., Salamé R., Salmon E., Kasparian J., Bergé L., Champeaux S., Guet C., Blanchot N., Bonville O., Boscheron A., Canal P., Castaldi M., Hartmann O., Lepage C., Marmande L., Mazataud E., Mennerat G., Patissou L., Prevot V., Raffestin D., Ribolzi J. *Appl. Phys Lett.*, **90**, 151106 (2007).
20. Kasparian J., Ackermann R., André Y.-B., Méchain G., Mejean G., Prade B., Rohwetter P., Salmon E., Stelmaszczyk K., Yu J., Mysyrowicz A., Sauerbrey R., Wöste L., Wolf J.-P. *Opt. Express*, **16**, 5757 (2008).

21. Dormidonov A.E., Valuev V.V., Dmitriev V.L., Shlenov S.A., Kandidov V.P. *Proc. SPIE Int. Soc. Opt. Eng.*, **6733**, 67332S (2007).
22. Chateauneuf M., Payeur S., Dubois J., Kieffer J.-C. *Appl. Phys. Lett.*, **92**, 091104 (2008).
23. Lukin V.P., Fortes B.V. *Adaptivnoe formirovanie puchkov i izobrazhenii v atmosfere* (Adaptive Formation of Beams and Images in Atmosphere) (Novosibirsk: Siberian Division, RAS, 1999).
24. Happer W., MacDonald G.J., Max C.E., Dyson F.J. *J. Opt. Soc. Am. A*, **11**, 263 (1994).
25. Thompson L.A., Castle R.M. *Opt. Lett.*, **17**, 1485 (1992).
26. Tracy A.J., Hankla A.K., Lopez C.A., Sadighi D.C., Rogers N., Groff K., McKinnie I.T., d'Orgeville C. *Proc. SPIE Int. Soc. Opt. Eng.*, **5490**, 998 (2004).
27. Wille H., Rodrigues M., Kasparian J., Mondelain D., Yu J., Mysyrowicz A., Sauerbrey R., Wolf J.P., Wöste L. *Europ. Phys. J. Appl. Phys.*, **20**, 183 (2002).
28. Méchain G., D'Amico C., André Y.-B., Tzortzakis S., Franco M., Prade B., Mysyrowicz A., Couairon A., Salmon E., Sauerbrey R. *Opt. Commun.*, **247**, 171 (2005).
29. Feng W., Lin L., Wang W., Li R., Xu Z. *Chin. Opt. Lett.*, **5**, S166 (2007).
30. Zemlyanov A.A., Geints Yu.E. *Opt. Atmos. Okean.*, **18**, 868 (2005).
31. http://www.grc.nasa.gov/WWW/K-12/airplane/atmosmet.html.
32. Andrews L.C., Phillips R.L. *Laser Beam Propagation Through Random Media* (Bellingham, Wash.: SPIE Opt. Eng. Press, 1998).
33. Shlenov S.A., Kandidov V.P. *Opt. Atmos. Okean.*, **17**, 630 (2004).
34. Zuev V.E., Banakh V.A., Pokasov V.V. *Optika turbulentnoi atmosfery* (Optics of Turbulent Atmosphere) (Leiningrad: Gidrometeoizdat, 1988).
35. Marburger J.H. *Prog. Quantum Electron.*, **4**, 35 (1975).
36. Fedorov V.Yu., Kandidov V.P. *Opt. Spektrosk.*, **105**, 306 (2008).
37. *Spravochnik po lazeram* (Handbook on Lasers) (Moscow: Sov. Radio, 1978) Vol. 1.
38. Gordienko V.M., Grechin S.S., Ivanov A.A., Podshivalov A.A. *Kvantovaya Elektron.*, **35**, 525 (2005) [*Quantum Electron.*, **35**, 525 (2005)].
39. Begishev I.A., Kalashnikov M., Karpov V., Nickles P., Schonnagel H. *J. Opt. Soc. Am. B*, **21**, 318 (2004).
40. Chong A., Renninger W.H., Wise F.W. *J. Opt. Soc. Am. B*, **25**, 140 (2008).
41. Akhmanov S.A., Gordienko V.M., Dzhidzhoev M.S., Krayushkin S.V., Platonenko V.T., Popov V.K. *Kvantovaya Elektron.*, **13**, 1957 (1986) [*Sov. J. Quantum Electron.*, **16**, 1291 (1986)].